JEAP

ISSN: 2525-815X

Journal of Environmental Analysis and Progress

10.24221/jeap.9.3.2024.6078.188-195

Desulfurization of coal pyrite tailings with ozone

Elcio Angioletto[a,b], Thauan Gomes[c], Eduardo Scheffer Magnus[a], Agenor de Noni Júnior[d], Elidio Angioletto[a,b]

[a] Universidade do Extremo Sul Catarinense-UNESC, Laboratório de Desenvolvimento de Biomateriais e Materiais Antimicrobianos-LADEBIMA. Av. Universitária, n. 1105, Criciúma, Santa Catarina, Brasil. CEP: 88806-000. E-mail: elcio36@gmail.com, eduardo.magnus99@gmail.com.

[b] UNESC, Programa de Pós-Graduação em Ciência e Engenharia de Materiais-PPGCEM. E-mail: ean@unesc.net.

[c] Instituto Federal de Santa Catarina-IFSC, Câmpus Gaspar. Rua Adriano Kormann, n. 510, Gaspar, Santa Catarina, Brasil. CEP: 89111-009. E-mail: thauan.gomes@ifsc.edu.br.

[d] Universidade Federal de Santa Catarina-UFSC, Departamento de Engenharia Química e Engenharia de Alimentos. Rua Eng. Agronômico Andrei Cristian Ferreira, s/n, Florianópolis, Santa Catarina, Brasil. CEP: 88040-900. E-mail: agenor.junior@ufsc.br.

ARTICLE INFO

Received 25 Jul 2023
Accepted 02 Aug 2024
Published 12 Aug 2024

ABSTRACT

Mining is an important sector of the economy, and in the southern region of Brazil, coal mining stands out. This activity generates waste with a high pyritic content, which causes environmental problems such as acid mine drainage (AMD). Therefore, studies that aim to beneficiate or treat this waste are highly relevant. In this study, an alternative for desulfurizing pyritic waste using ozone was investigated. Ozone treatment of mining tailings suspension was evaluated as a new strategy for sulfur removal. Particle size analysis, sulfate content, ferrous ion concentration (and total iron), pH, Eh, conductivity, and X-ray fluorescence were performed. Furthermore, a kinetic analysis of ozone consumption was established. The behavior of sulfate and hydrogen ion concentrations indicates that sulfuric acid is the main reaction product, and conductivity suggests that ion release is continuous over the ozonation time. Reaction kinetics with $\alpha \cong 1.2$ was found for ozone depletion, which aids in predicting the dosage to be applied on a larger scale. This study contributes to the search for alternatives for treating pyritic waste and contributes to the understanding of the reaction rate of ozone consumption in this type of reaction.

Keywords: Oxidation, sulfates, ozonation.

Introduction

The mining industry makes a substantial contribution to the economy of many regions around the world. However, it also causes environmental disadvantages (Anawar, 2015; Park et al., 2019; Gomes et al., 2022a). The main environmental issue associated with mining activities is the formation of acid mine drainage (AMD). This occurs when sulfide minerals (previously buried) are exposed to natural oxidizing agents such as air, water, and microorganisms (Akcil & Koldas, 2006; Alakangas et al., 2013; Parbhakar-Fox & Lottermoser, 2015). The most common mineral that generates AMD is pyrite (FeS_2), which, despite having low economic value, is abundantly present in ores such as coal, copper, iron, and uranium (Chandra & Gerson, 2010; Lv et al., 2021). In Santa Catarina alone, over 11 million tons of coal were mined in 2020 and 2021 (SIECESC, 2021). This generates a significant amount of waste. There are approximately 300 million tons of coal waste in the country's southern region, with significant amounts of sulfur (Amaral Filho et al., 2013).

Therefore, alternatives for processing mining waste are of high relevance. Research endeavors focused on enhancing the sulfur concentration in coal waste via jigging have been undertaken (Ambrós, 2020). Additionally, the pyrite present in the coal mining waste can be roasted to produce iron oxides, and sulfur can be retained in a solution with sodium or calcium hydroxide (Wang et al., 2020; Gomes et al., 2022b). Another possibility is the oxidation of the pyritic content to form ferrous sulfate (Peterson, 2008). For this purpose, alternatives using grinding or heating have been proposed (Santos et al., 2016). In these cases, the oxidant used is oxygen (O_2).

However, this oxidant poses limitations in converting pyrite to ferrous sulfate because its oxidation potential is low compared to other oxidants (such as permanganates). Furthermore, the solubility of oxygen in an aqueous medium is negatively affected by temperature, which is proportional to the reaction rate (Hwang et al., 1987). Equations 1 and 2 are commonly cited for oxidizing pyrite in an aqueous medium with oxygen.

$$2\ FeS_2 + 7\ O_2 + 2\ H_2O \rightarrow 2\ FeSO_4 + 2\ H_2SO_4 \quad \text{Eq. (1)}$$

$$4\ FeS_2 + 15\ O_2 + 2\ H_2O \rightarrow 2\ Fe_2(SO_4) + 2\ H_2SO_4 \quad \text{Eq.(2)}$$

By analogy, Hwang et al. (1987) suggested representing the ozonation of pyrite based on these reactions, according to Equations 3 and 4.

$$3\ FeS_2 + 7\ O_3 + 3\ H_2O \rightarrow 3\ FeSO_4 + 3\ H_2SO_4 \quad \text{Eq. (3)}$$

$$2\ FeS_2 + 5\ O_3 + H_2O \rightarrow Fe_2(SO_4)_3 + H_2SO_4 \quad \text{Eq. (4)}$$

It is noticeable that these equations assume the complete reaction of all three oxygen atoms in ozone (O_3). In practice, the oxidation of pyrite by ozone likely involves the production of O_2 as a byproduct, as demonstrated by Equation 5.

$$FeS_2 + 7\ O_3 + H_2O \rightarrow FeSO_4 + H_2SO_4 + 7\ O_2 \quad \text{Eq. (5)}$$

Then, there is additional oxygen oxidation, as shown in Equation 1. The addition of Equations 1 and 5 results in Equation 3. If the reaction shown in Equation 5 is relatively fast compared to the reaction in Equation 1, then the reaction in Equation 5 could predominate, and the ozone/pyrite molar ratio should approach 7. This was demonstrated by Rodríguez-Rodríguez, Nava-Alonso & Uribe-Salas (2018), where the pyrite-ozone reaction system was studied and found to be three orders of magnitude more reactive compared to the pyrite-oxygen system.

Furthermore, the stoichiometric problem may be more complex, as other sulfur intermediate reaction products may be formed, especially when considering the variable composition of mining waste. The ozone/pyrite molar ratio can vary over time within a range of 2.33 to 7, with ozone demand being even higher due to losses from undesirable reactions and/or self-decomposition (Hwang et al., 1987; Gomes et al., 2019).

Therefore, studying the ozonation of pyritic waste is challenging from the standpoint of establishing reaction mechanisms. Even so, ozone is an alternative oxidant of great interest because it stands out for its high oxidation potential, low cost, and no addition of residues. Thus, this study aimed to investigate the oxidation of pyritic waste by ozone on a laboratory scale, evaluating the potential generation of sulfates as a pyrite processing route.

Material and Methods

Kinetic analysis: ozone consumption

A laboratory reactor with inlet and outlet ports positioned at the top was used, as shown in Figure 1. 10 g of coal mining waste (milled, mesh sieve with an aperture of 0.077 mm) and 1 L of water was added to promote an aqueous suspension. Ozone was generated from oxygen concentration using a Brazil Ozônio® generator, model BRO3-PLUS2.1. The oxygen flow rate (v) was controlled by a flowmeter [brand: Soldax Soldas]. A flow rate of 12 L·min^{-1} was employed. An ozone analyzer continuously measured ozone generation [BMT 964 BT; Bmt Messtechnik GmbH]. The ozone concentration (C_{O_3}) was used at different levels: 10, 12, and 18 g·Nm^{-3}. Ozone was bubbled through a common porous stone connected to the supply hose. In addition to bubbling, a magnetic stirrer was employed to prevent sedimentation during ozonation. The experiment was conducted at 25˚C.

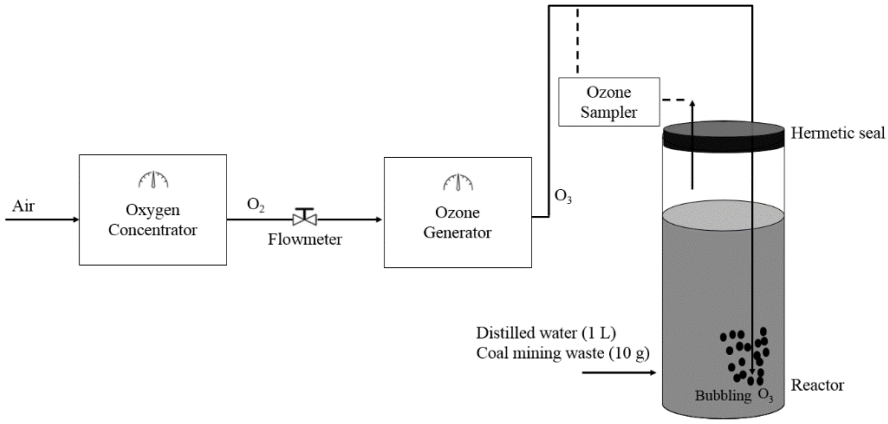

Figure 1. Experimental scheme. Font: Angioletto et al. (2024).

The ozone analyzer was connected to the reactor outlet, and the concentration was monitored over time (t). Reaction times of 1, 2, 4, and 8 h were established. Based on the data for the steady state, ozone consumption was evaluated. Equation 6 was used to determine the reaction rate.

$$R_{O_3} = \frac{F_{O_3,out} - F_{O_3,in}}{V_r} \quad \text{Eq. (6)}$$

In this equation, R_{O_3} represents the reaction rate (mol L^{-1} min^{-1}), and V_r is the reactor volume (L). $F_{O_3,in}$ and $F_{O_3,out}$ are the molar flow rates of ozone at the inlet and outlet (mol·min^{-1}), respectively. Equation 7 establishes the determination of these flow rates.

$$F_{O_3} = C_{O_3}.v \quad \text{Eq. (7)}$$

In Equation 7, C_{O_3} represents the ozone concentration (mol· L^{-1}), and v is the volumetric flow rate (L·min^{-1}). Since the mining waste contains numerous reactive species, the following reaction was considered, as shown in Equations 8 and 9.

O_3 + coal mining waste→ products Eq. (8)

$$-R_{O_3} = k_{O_3} \cdot \left(C_{O_{3,in}}\right)^{\alpha} \quad \text{Eq. (9)}$$

This is a common strategy for evaluating ozone decomposition (including self-decomposition) (Gomes et al., 2019; Souza et al., 2021). The obtained rate law accounts for the reactions associated with ozone decomposition. In Equation 9, k_{O_3} and α represent the specific reaction rate and reaction order, respectively. $C_{O_{3,in}}$ is the ozone concentration applied at the inlet. The ozone decomposition rate was determined by linearizing Equation 9, as demonstrated in Equation 10.

$$Ln\left(-R_{O_3}\right) = ln\, k_{O_3} + \alpha \cdot Ln\, C_{O_{3,in}} \quad \text{Eq. (10)}$$

After ozonation, the aqueous suspension was vacuum filtered, generating two "products": solid and liquid. These were evaluated for desulfurization.

Desulfurization analysis

The solid product was characterized after ozonation via X-ray diffraction (Shimadzu® 6000 - CuKa radiation λ = 1.5406 Å, 25 kV, 25 mA). Additionally, elemental analysis via X-ray fluorescence (Model: EDX 7000, brand: Shimadzu), following the semi-quantitative method of oxides for solid and powder samples, was performed. Furthermore, the average particle size before and after the reaction was measured using a Cilas 1064 laser analyzer.

The liquid product was analyzed for the presence of 1) sulfates through ion chromatography using the EPA 300.1/SMEWW methodology (Standard Methods for the Examination of Water and Wastewater 4110B); 2) total iron via Inductively Coupled Plasma Optical Emission Spectrometry (ICP-OES 720; Agilent Technologies, Santa Clara, CA, USA), using the SMEWW method 3120B; and 3) ferrous ion through redox titration using potassium permanganate. Additionally, a multiparameter analyzer (YSI-Pro Plus) was used to determine pH, Eh (V), and conductivity (µS·cm^{-1}). For this part of the study, a reaction time of 4 h was used.

Redox titration for the determination of ferrous ion

This analytical method uses a standard potassium permanganate (KMnO4) solution to determine the amount of Fe^{2+} present in the solution (Kaufman & Devoe, 1988).

The permanganate ion is reduced to a manganese ion in the acidic solution related to Equation 11.

$MnO_4^- + 8H^+ + 5e^- \rightarrow Mn^{+2} + 4\ H_2O$ Eq. (11)

Equation 11 shows a reaction that requires five electrons and eight hydrogen ions. However, Equation 12 shows that only one electron is needed to reduce Fe^{3+} to Fe^{2+}.

$Fe^{3+} + e^- \rightarrow Fe^{2+}$ Eq. (12)

Therefore, one mole of MnO_4^- (oxidizing agent) reacts with five moles of Fe^{2+} (reducing agent) to form five moles of Fe^{3+} and one mole of Mn^{2+}, as shown in Equation 13.

$MnO_4^- + 5\ Fe^{2+} + 8H^+ \rightarrow 5\ Fe^{3+} + Mn^{2+} + 4H_2O$ Eq.(13)

The 1:5 molar ratio between the amounts of MnO_4^- and Fe^{2+} consumed establishes the stoichiometry for determining the concentration of Fe^{2+}.

As mentioned, the KMnO4 solution was prepared using sulfuric acid as the diluent. This ensured the medium's acidification for a complete reaction. A solution of ferrous ions with a known concentration standardized the potassium permanganate solution (~0.05 M). Then, the liquid samples resulting from desulfurization were titrated. The change in color of the solution established the endpoint.

Results and Discussion

Kinetic analysis of ozone consumption

Figure 2A shows the time-dependent ozone concentration, while Figure 2B demonstrates the application of Equation 6 to assess the reaction rate (R_{O_3}) as a function of time.

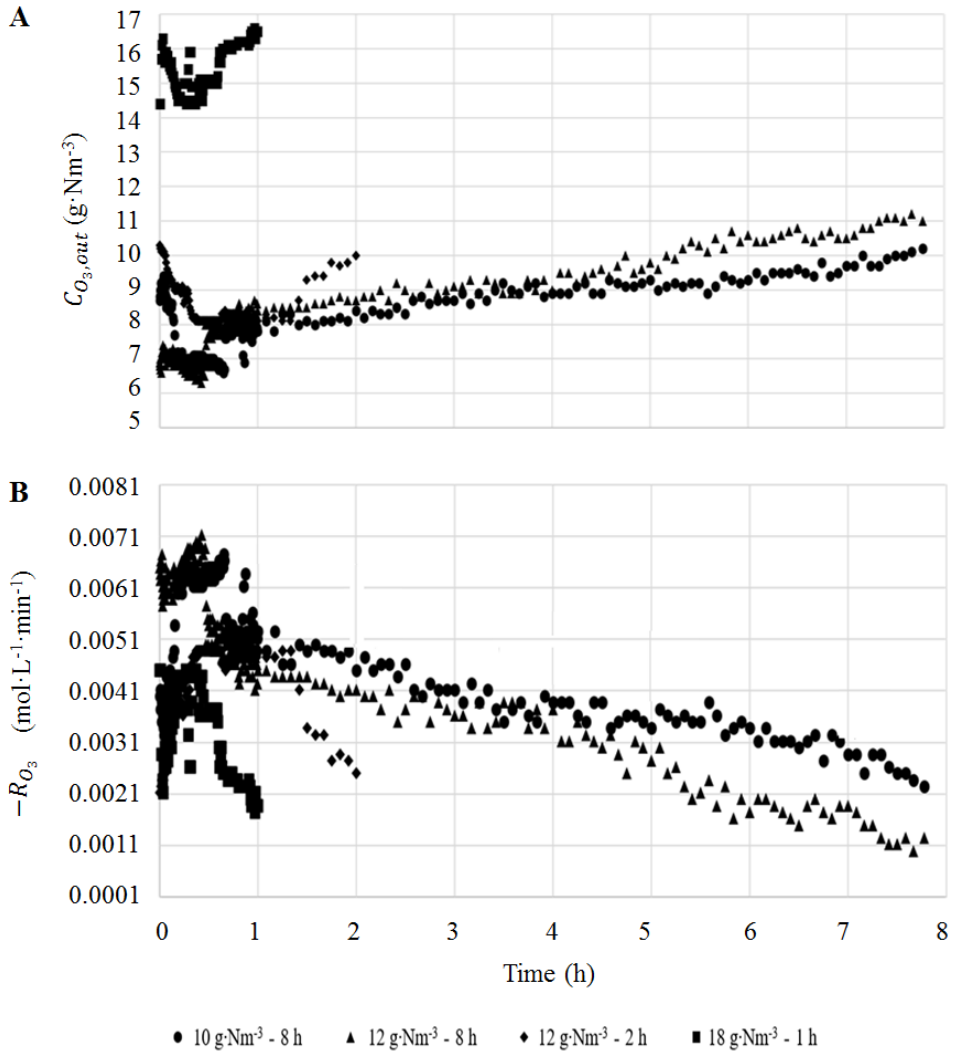

Figure 2. Ozone concentration (A) and reaction rate (B) as a function of time. Font: Angioletto et al. (2024).

It was observed that the ozone concentration at the reactor outlet increases over time. This can be explained by the continuous reaction of the numerous chemical species in the mining waste as time progresses.

Hwang et al. (1987) proposed the unreacted core model to describe the kinetics of pyrite ozonation in aqueous suspension. This is consistent with the present study, as the behavior of pyritic waste can also conform to this type of kinetics. Some authors describe possible mechanisms for ozone attack on pyrite, with a passivation layer forming a common observation (Bessho et al., 2011; Kollias et al., 2014). This would be in line with the behavior of the reaction rate shown in Figure 2B; however, Rodríguez-Rodríguez, Nava-Alonso & Uribe-Salas (2018) in a similar study observed that the application of ozone leads to the absence of a passive layer on the pyrite surface. Corroborating, Lv et al. (2021) used ozone to eliminate a passivation layer; their results showed that ozone remarkably increased the electrochemical reactivity of passivated pyrite. This indicates that ozone enhanced the dissolution of passivated pyrite by destroying the passivation layer.

Additionally, the average particle size of the waste before and after ozonation remains stable (18.55 µm before and 17.74 µm after), indicating minimal particle wear during the process. The formation of oxides on the surface explains the decrease in the ozone consumption rate over time.

In this study, the reaction mechanism was not investigated; instead, the focus was on the ozone consumption rate. This is because the practical significance lies in determining the ozone dosage required for pyrite desulfurization. Thus, our kinetic model accounted for ozone depletion.

The application of Equation 10 is illustrated in Figure 3. The linear fit with an R^2 value of 0.96 indicates that the linearization shown in Equation 14 is adequate.

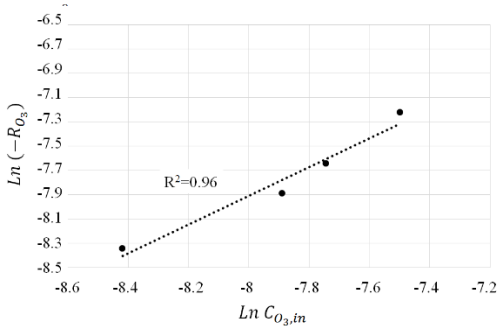

Figure 3. $Ln\,(-R_{O_3})$ *versus* $Ln\,C_{O_3,in}$. Font: Angioletto et al. (2024).

$$Ln\,(-R_{O_3}) = 1.55 + 1.18 \cdot Ln\,C_{O_3,in} \qquad \text{Eq. (14)}$$

Thus, the reaction kinetics behavior demonstrates α≅1.2, and the proposed rate law is shown in Equation 15.

$$R_{O_3} = -4.7 \cdot C_{O_3,in}^{\,1,2} \qquad \text{Eq. (15)}$$

Gomes et al. (2022a) assessed that the reaction rate depends on the amount of water in a coal mining waste pile (without comminution). They observed, for example, that when saturation is at its maximum, a rate of $-0.37 \cdot C_{O_3,in}^{\,0.43}$ is observed. The rate found in this study is higher (due to higher values of k_{O_3}, and α), and this can be understood because the reaction here was conducted with micrometric particles in suspension. In contrast, the mentioned study was an *in situ* application with naturally sized rocks.

Analysis of iron and sulfate generation evolution, pH, Eh, and conductivity

Table 1 illustrates the elemental composition of the pyritic waste obtained via X-ray fluorescence.

Table 1. Elementary analysis of coal mining waste. Font: Angioletto et al. (2024).

Element (Oxide)	Content (%)
SiO_2	62.55
Al_2O_3	29.12
Fe_2O_3	3.08
K_2O	2.08
TiO_2	1.53
MgO	0.297
SO_3	0.125
ZrO_2	0.065
ZnO	0.054
CuO	0.021
Rb_2O	0.013
NiO	0.009
SrO	0.008
Loss on ignition	1.05

The coal mining waste is predominantly composed of SiO_2 and Al_2O_3. A small amount of sulfur was also identified (qualitatively). This is inherent to the analysis, as a sample is pearled at a temperature at which sulfur volatilizes. Iron indicates a pyritic content, confirmed through X-ray diffraction, where pyrite (JCPDS: 42-1340) was observed.

Figure 4A illustrates that the concentration of ferrous ions increases over time.

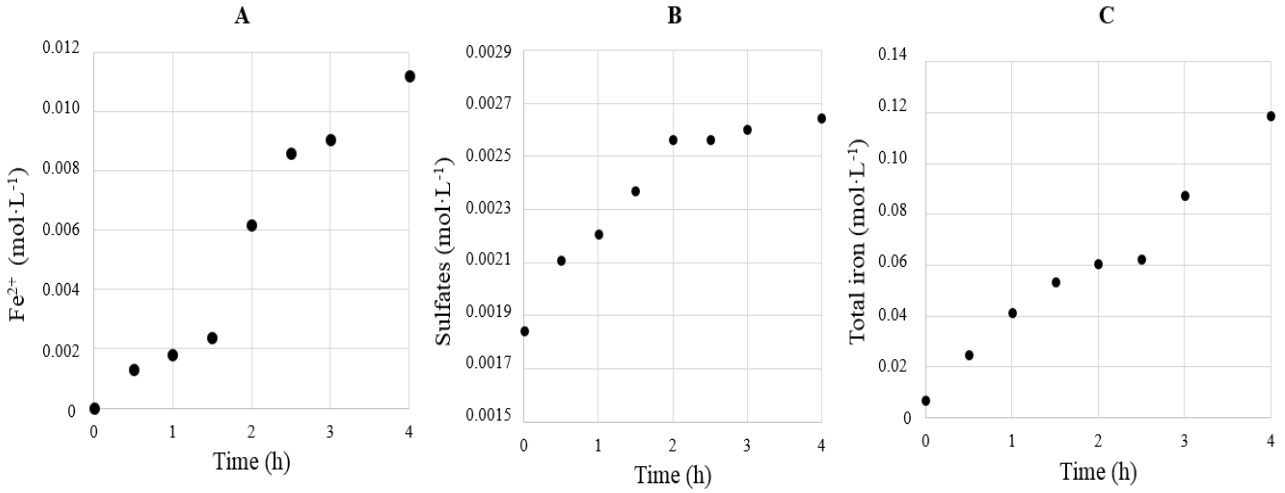

Figure 4. Ferrous ion (A) sulfates (B) and total iron (C) concentrations as a function of time. Font: Angioletto et al. (2024).

This follows Hwang et al. (1987), who suggested Equation 5 (shown in the introduction) as the established reaction. Therefore, the formation of ferrous sulfate is expected when the coal mining waste suspension is ozonized. This is corroborated by the analysis of sulfate content over time, as shown in Figure 4B. The sulfate content increased over time, reaching a maximum of 0.00265 mol·L^{-1}. However, the ferrous ion reaches a maximum of 0.0111 mol·L^{-1} at t = 4 h, with a continued upward trend. Since ferrous sulfate has a 1:1 ratio (mol of Fe^{2+}:mol of $SO4^{-2}$), the established ratio indicates that iron is present in forms other than sulfate. This is evidenced by the sample's analysis of total iron content, as shown in Figure 4C. In this case, the shape of this curve is like that found for the ferrous ion (Figure 4A). This indicates that the oxidation of iron (linked to sulfides) is occurring and does not end at t = 4 h. Since the formation of sulfates reaches a maximum at t = 2 h (Figure 4B), it is possible that the formation of ferrous sulfate ceases after this period, and other iron oxides are formed.

Figure 5 illustrates the monitoring of pH, Eh, and conductivity over time.

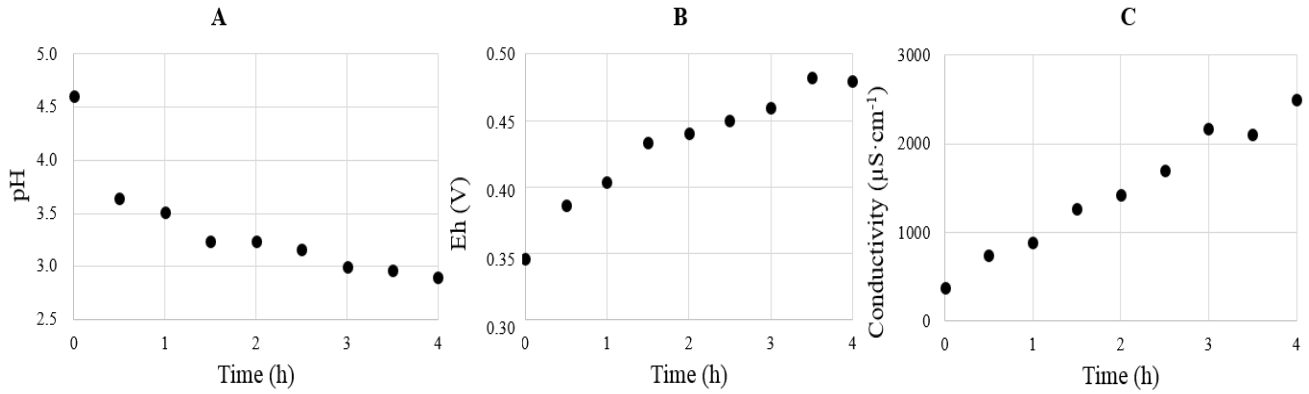

Figure 5. Monitoring of pH (A), Eh (B), and conductivity (C) as a function of time. Font: Angioletto et al. (2024).

It is known that desulfurization of coal mining waste by ozonation should result in the formation of sulfuric acid, as indicated by the reactions shown in Equations 3 and 4. Therefore, a decrease in pH over the reaction time is expected. At t = 4 h, a pH of 2.9 was found, indicating an H^+ concentration of 0.001259 mol·L^{-1}, which is consistent with the sulfate concentration found (0.00265 mol·L^{-1}) because the hydrogen/sulfate ratio in sulfuric acid is 2.

Additionally, the analysis of redox potential (Eh) supports the hypothesis of pyrite consumption in coal mining waste. Saria, Shimaoka & Miyawaki (2006) demonstrated that increased Eh is associated with increased pyrite consumption in leaching experiments without ozone. They found around 0.6 V after several days of exposing mining waste to water. It obtained a similar Eh value in just a few hours, highlighting the strong oxidative effect of ozone. Furthermore, conductivity (Figure 5C) indicates that desulfurization is also related to the dissolution of other minerals in the coal mining waste. This can be explained by observing the stabilization in sulfate content while conductivity does not exhibit the same behavior.

In addition to attacking the pyritic content (desulfurization), ozone causes prolonged reactions with the mineral matrix. Ozone favors a decrease in pH (by reacting with sulfides), causing the leaching of other minerals. This increases the number of dissolved metals in the liquid phase, which are then oxidized.

Although this study did not aim to establish a mechanism, it is plausible that desulfurization occurs faster than leaching of other mineral species, and the ozone dosage (application time) can be optimized for this purpose. Thus, the evaluated reaction kinetics can be used to estimate ozone consumption, and an analysis of the initial sulfide content in the coal mining waste should indicate the ozone required for desulfurization.

Conclusion

The oxidation of coal mining waste using bench-scale ozone treatment demonstrated the potential generation of sulfates as a processing route for this mineral residue.

Additionally, a data acquisition system for ozone concentration simultaneous to the process established a reaction kinetics with α≅1.2. The behavior of sulfate and hydrogen ion (H^+) concentrations indicated that sulfuric acid is the

main reaction product. Furthermore, the formation of ferrous sulfate occurs, which can be an alternative processing method for mining waste.

It was observed that desulfurization is also related to the solubilization of other minerals in the coal mining waste, requiring attention to undesired leaching.

This study presents a new alternative to using coal mining waste and contributes to environmental progress and chemical technology.

Acknowledgments

The authors thank the Conselho Nacional de Desenvolvimento Científico e Tecnológico (CNPq) for the scholarship to Elcio Angioletto and for funding the research.

References

Akcil, A.; Koldas, S. 2006. Acid Mine Drainage (AMD): causes, treatment and case studies. Journal of Cleaner Production, 14, 1139-1145. https://doi.org/10.1016/j.jclepro.2004.09.006

Alakangas, L.; Andersson, E.; Mueller, S. 2013. Neutralization/prevention of acid rock drainage using mixtures of alkaline by-products and sulfidic mine wastes. Environmental Science and Pollution Research, 20, 7907-7916. https://doi.org/10.1007/s11356-013-1838-z

Amaral Filho, J. R.; Schneider, I. A. H.; Brum, I. A. S. de.; Sampaio, C. H.; Miltzarek, G.; Schneider, C. 2013. Caracterização de um depósito de rejeitos para o gerenciamento integrado dos resíduos de mineração na região carbonífera de Santa Catarina, Brasil. Revista Escola de Minas, 66, 347-353. https://doi.org/10.1590/S0370-44672013000300012

Ambrós, W. M. 2020. Jigging: A Review of Fundamentals and Future Directions. Minerals, 10, 998. https://doi.org/10.3390/min10110998

Anawar, H. M. 2015. Sustainable rehabilitation of mining waste and acid mine drainage using geochemistry, mine type, mineralogy, texture, ore extraction and climate knowledge. Journal of Environmental Management, 158, 111-121. https://doi.org/https://doi.org/10.1016/j.jenvman.2015.04.045

Bessho, M.; Wajima, T.; Ida, T.; Nishiyama, T. 2011. Experimental study on prevention of acid mine drainage by silica coating of pyrite waste rocks with amorphous silica solution. Environmental Earth Sciences, 64, 311-318. https://doi.org/10.1007/s12665-010-0848-0

Chandra, A. P.; Gerson, A. R. 2010. Surface Science Reports The mechanisms of pyrite oxidation and leaching: A fundamental perspective. Surface Science Reports, 65, 293-315. https://doi.org/10.1016/j.surfrep.2010.08.003

Gomes, T.; Angioletto, E.; Quadri, M. B.; Cardoso, W.A. 2019. Ozone Propagation in Sterile Waste Piles from Uranium Mining: Modeling and Experimental Validation. Transport in Porous Media, 127, 157-170. https://doi.org/10.1007/s11242-018-1184-1

Gomes, T.; Angioletto, E.; Quadri, M. B.; Cargnin, M.; Souza, H. M. 2022a. Acceleration of acid mine drainage generation with ozone and hydrogen peroxide: Kinetic leach column test and oxidant propagation modeling. Minerals Engineering, 175, 107282. https://doi.org/10.1016/j.mineng.2021.107282

Gomes, T.; Rosa, R.; Cargnin, M.; Quadri, M. B.; Peterson, M.; Oliveira, C. M.; Rabelo N. R.; Angioletto, E. 2022b. Pyrite roasting in modified fluidized bed: Experimental and modeling analysis. Chemical Engineering Science, 261, 117977. https://doi.org/https://doi.org/10.1016/j.ces.2022.117977

Hwang, C. C.; Streeter, R. C.; Young, R. K.; Shah, Y. T. 1987. Kinetics of the ozonation of pyrite in aqueous suspension. Fuel, 66, 1574-1578. https://doi.org/10.1016/0016-2361(87)90022-6

Kaufman, S.; Devoe, H. 1988. Iron analysis by redox titration: A general chemistry experiment. Journal of Chemical Education, 65, 183. https://doi.org/10.1021/ed065p183

Kollias, K.; Mylona, E.; Adam, K.; Papassiopi, N.; Xenidis, A. 2014. Suppression of Pyrite Oxidation by Surface Silica Coating. Journal of Geoscience and Environment Protection, 02, 37-43. https://doi.org/10.4236/gep.2014.24006

Lv, X.; Zhao, H.; Zhang, Y.; Yan, Z.; Zhao, Y.; Zheng, H.; Liu, W.; Xie, J.; Qiu, G. 2021. Active destruction of pyrite passivation by ozone oxidation of a biotic leaching system. Chemosphere, 277, 130335. https://doi.org/https://doi.org/10.1016/j.chemosphere.2021.130335

Parbhakar-Fox, A.; Lottermoser, B. G. 2015. A critical review of acid rock drainage prediction methods and practices. Minerals Engineering, 82, 107-124. https://doi.org/10.1016/j.mineng.2015.03.015

Park, I.; Tabelin, C. B.; Jeon, S.; Li, X.; Seno, K.; Ito, M.; Hiroyoshi, N. 2019. A review of recent strategies for acid mine drainage prevention and mine tailings recycling. Chemosphere, 219, 588-606. https://doi.org/https://doi.org/10.1016/j.chemosphere.2018.11.053

Peterson, M. 2008. Produção de sulfato ferroso a partir da pirita: desenvolvimento sustentável. Doctoral thesis. Universidade Federal de Santa Catarina, Florianópolis, Santa Catarina, Brasil. 128p.

Rodríguez-Rodríguez, C.; Nava-Alonso, F.; Uribe-Salas, A. 2018. Pyrite oxidation with ozone: stoichiometry and kinetics. Canadian Metallurgical Quarterly, 57, 294-303. https://doi.org/10.1080/00084433.2018.1460437

Santos, E. C.; Silva, J. C. M.; Duarte, H. A. 2016. Pyrite Oxidation Mechanism by Oxygen in Aqueous Medium. The Journal of Physical Chemistry C, 120, 2760-2768. https://doi.org/10.1021/acs.jpcc.5b10949

Saria, L.; Shimaoka, T.; Miyawaki, K. 2006. Leaching of heavy metals in acid mine drainage. Waste Management & Research, 24, 134-140. https://doi.org/10.1177/0734242X06063052

Souza, H. M.; Savi, G. D.; Gomes, T.; Cardoso, W. A.; Cargnin, M.; Angioletto, E. 2021. Ozone Application in COVID-19 Triage Areas and Its Efficiency of Microbial Decontamination. Ozone: Science & Engineering, 43, 306-316. https://doi.org/10.1080/01919512.2021.1908880

SIECESC. 2021. (Sindicato da Indústria de Extração de Carvão do Estado de Santa Catarina, Carvão Mineral) – Dados Estatísticos – Ano: 2020, 2021. Available at: http://www.siecesc.com.br/dados_estatisticos. Access at: 20/06/2023.

Wang, T.; Zhang, H.; Yang, H.; Lv, J. 2020. Oxidation mechanism of pyrite concentrates (PCs) under typical circulating fluidized bed (CFB) roasting conditions and design principles of PCs' CFB roaster. Chemical Engineering and Processing - Process Intensification, 153, 107944. https://doi.org/https://doi.org/10.1016/j.cep.2020.107944